

## SOURCE ROCK POTENTIAL AND DEPOSITIONAL ENVIRONMENT OF UPPER PERMIAN OIL SHALES OF THE LUCAOGOU FORMATION IN THE SOUTHEASTERN JUNGGAR BASIN, NORTHWEST CHINA

YUAN GAO<sup>(a,d)</sup>, YONGLI WANG<sup>(b)\*</sup>, PING'AN PENG<sup>(a)\*</sup>,  
DAXIANG HE<sup>(c)</sup>, GEN WANG<sup>(b)</sup>, ZIXIANG WANG<sup>(b)</sup>,  
PEI MENG<sup>(b)</sup>, ZEPENG SUN<sup>(b)</sup>, JUNCHENG GONG<sup>(b)</sup>,  
HUI YANG<sup>(b)</sup>, YINGQIN WU<sup>(b)</sup>, YOUXIAO WANG<sup>(b)</sup>

- <sup>(a)</sup> State Key Laboratory of Organic Geochemistry, Guangzhou Institute of Geochemistry, Chinese Academy of Sciences, Guangzhou 510640, China
- <sup>(b)</sup> Gansu Provincial Key Laboratory of Petroleum Resources, Key Laboratory of Petroleum Resources Research, Institute of Geology and Geophysics, Chinese Academy of Sciences, Lanzhou 730000, China
- <sup>(c)</sup> State Key Laboratory of Petroleum Resources and Prospecting, College of Geosciences, China University of Petroleum, Beijing 102249, China
- <sup>(d)</sup> University of Chinese Academy of Sciences, Beijing 100049, China

**Abstract.** Oil shales from the Yamalikeshan (YML), Shuimogou (SMG) and Sangonghe (SGH) sections of the Lucaogou Formation in the southeastern Junggar Basin, Northwest China are rich in organic matter and have high hydrocarbon generation potential, as shown by bulk Rock-Eval and chloroform extract analyses. The contrast in organic composition between the oil shales implies that Sangonghe is the richest hydrocarbon source rock section in the studied area in the Junggar Basin. The distribution of biomarkers and organic carbon isotope parameters indicate that oil shales of the Lucaogou Formation were deposited in a cool and humid paleoclimate and that some layers were partly subjected to microbial modification. In addition, the Sangonghe oil shale suggested a strongly reducing depositional environment, deeper and higher-salinity lake waters and a higher input of lower aquatic organisms compared with oil shales of the other two sections. Therefore we conclude that brackish reducing deep lakes were favourable for the development of petroleum source rocks. Ketones and aldehydes were identified in two Yamalikeshan oil shale samples, while ketones and fatty acid methyl esters (FAMEs) were found in the other two samples from the same section. In none of the samples the co-existence of all three compounds was established. The

---

\* Corresponding author: e-mail [wyl16800@lzb.ac.cn](mailto:wyl16800@lzb.ac.cn), [pinganp@gig.ac.cn](mailto:pinganp@gig.ac.cn)

*unique occurrence of aldehydes and fatty acid methyl esters may imply the varying depositional environment of the Yamalikeshan section.*

**Keywords:** *Lucaogou Formation, Upper Permian, aldehyde, fatty acid methyl esters, Junggar Basin, biomarkers, organic carbon isotopes.*

## 1. Introduction

The Upper Permian oil shales of the Lucaogou Formation outcropping in the southeastern Junggar Basin, Northwest China were long ago identified and reported to contain abundant organic matter and have considerable thickness [1–4]. Several authors have ranked these silicic mudstones among the thickest and richest petroleum source rock intervals in the world [2, 3]. Carroll et al. [4] studied two Upper Permian sections in the western foothill of Bogda Mountain identified as the Tianchi and Urumuqi sections, which included rocks (from the oldest to the youngest) of the Jingjingzigou, Lucaogou and Hongyanchi formations. Li [5] and Tao et al. [6] documented several Lucaogou Formation profiles in the eastern part of the foothill of Bogda Mountain. The Upper Permian rocks of the Junggar Basin are exclusively lacustrine deposits, based on fossil evidence, metallogenic characteristics, sedimentary facies, as well as macro-, trace and rare earth elements analyses [7–13].

Although several investigations have been carried out on Lucaogou oil shales in the Junggar Basin, they chiefly concerned with the sedimentary environment by using elemental geochemical methods [5–7, 9, 10, 13]. The study area of most of these articles was the eastern part of the foothill of Bogda Mountain. However, some researchers conducted a comprehensive study of oil shales in the western part of Bogda Mountain to describe their sedimentary and organic geochemical characteristics [4, 14]. In the present work, oil shales from three sections of the Lucaogou Formation in the western part of Bogda Mountain – Yamalikeshan (YMS), Shuimogou (SMG) and Sangonghe (SGH) – were analysed using organic geochemistry methods, including biomarkers and total organic carbon isotope, to define the source rock quality, depositional environment and organic matter input. We focus on the comparison of the sedimentary environments, organic material inputs and potentials for hydrocarbon source rock exploration of oil shales from the said sections of the Lucaogou Formation. Moreover, organic geochemistry evidence of the paleogeographic relations between the sections is presented. This is also the first study ever to report the occurrence of oxygenated compounds in oil shales in the area investigated.

### 1.1. Geological setting

Located in the northern part of the Xinjiang Uygur Autonomous Region, Northwest China, the Junggar Basin is a triangular foreland deposit covering an area of approximately 137,000 km<sup>2</sup> [15]. The lateral extent of the Junggar

Basin is marked by Palaeozoic fold mountain systems on its northwestern, northeastern and southern edges (Fig. 1a). The basement of the basin appears to be accretionary oceanic rocks and island arcs that were stabilized as late as the Carboniferous to the Early Permian [14, 16]. The Junggar Basin is a giant polycyclic superposition basin with multiple sets of hydrocarbon source rocks, with the Upper Permian source rocks, which are primarily exposed at the northern foothill of Bogda Mountain and the front of Kelameili Mountain, being the most important among them [11].

The study areas, i.e. the Yamalikeshan, Shuimogou and Sangonghe sections (Fig. 1b, simplified from [17, 18]), which are located at the northern foothill of Bogda Mountain in the southeastern part of the Junggar Basin, went through multiple stages of tectonic movement and intense folding. During the Late Carboniferous, the basin was still in the stage of peripheral foreland basins. The depositional environment evolved from a shallow marine system in the Carboniferous to a coastal system in the Early Permian [19, 20]. The Middle and Upper Permian series deposited in the alluvial fan-fluvial to lacustrine environment are mainly non-marine clastic sediments [21, 22]. During the Late Permian the Bogda Mountain area was in the extension rift setting and a deep to semi-deep lacustrine depositional environment [4, 9, 22, 23] (Fig. 2, modified after [10, 24]). In addition to the provenance derived from the Late Paleozoic magmatic belt in the North Tianshan block, the other major source of the Bogda area was synchronous pyroclastic material [23, 25]. During the Middle-Late Triassic to the Early Jurassic period, the Bogda area was in the weak extension and stable subsidence stage, and the sedimentary facies include braided river delta and lacustrine facies. Bogda Mountain began to uplift during the Middle-Late Jurassic and became a major provenance of the submountain region [23, 25]. Due to the huge south-north compressive stress caused by the India-Asia collision, the Bogda area uplifted rapidly and greatly since the Neogene. The Upper Permian oil shales at the northern foothill of the mountain were exposed and formed a large-scale oil shale distribution zone (Figs. 1b–c, modified after [19]), with a length of approximately 143 km and width of 9–15 km [1, 10].

Oil shales of the Lucaogou Formation in the Bogda area were mainly deposited in a deep to semi-deep lacustrine depositional environment, with the provenance derived from the Late Paleozoic magmatic belt in the North Tianshan block (Fig. 2). The Lucaogou Formation can be divided into three segments corresponding to three sedimentary systems (Fig. 3) [10, 13]. Segment 1 consists of siltstone interbedded with sandstone in the lower part and siltstone in the upper part, deposited in a strand shallow lake environment during the period of the lowstand systems tract. Segment 2 mainly consists of sandy shale and sandstone interbedded with sandy oil shale, and was deposited in shallow to semi-deep lake facies during the period of the transgressive stand system. Segment 3 was deposited in a semi-deep to deep

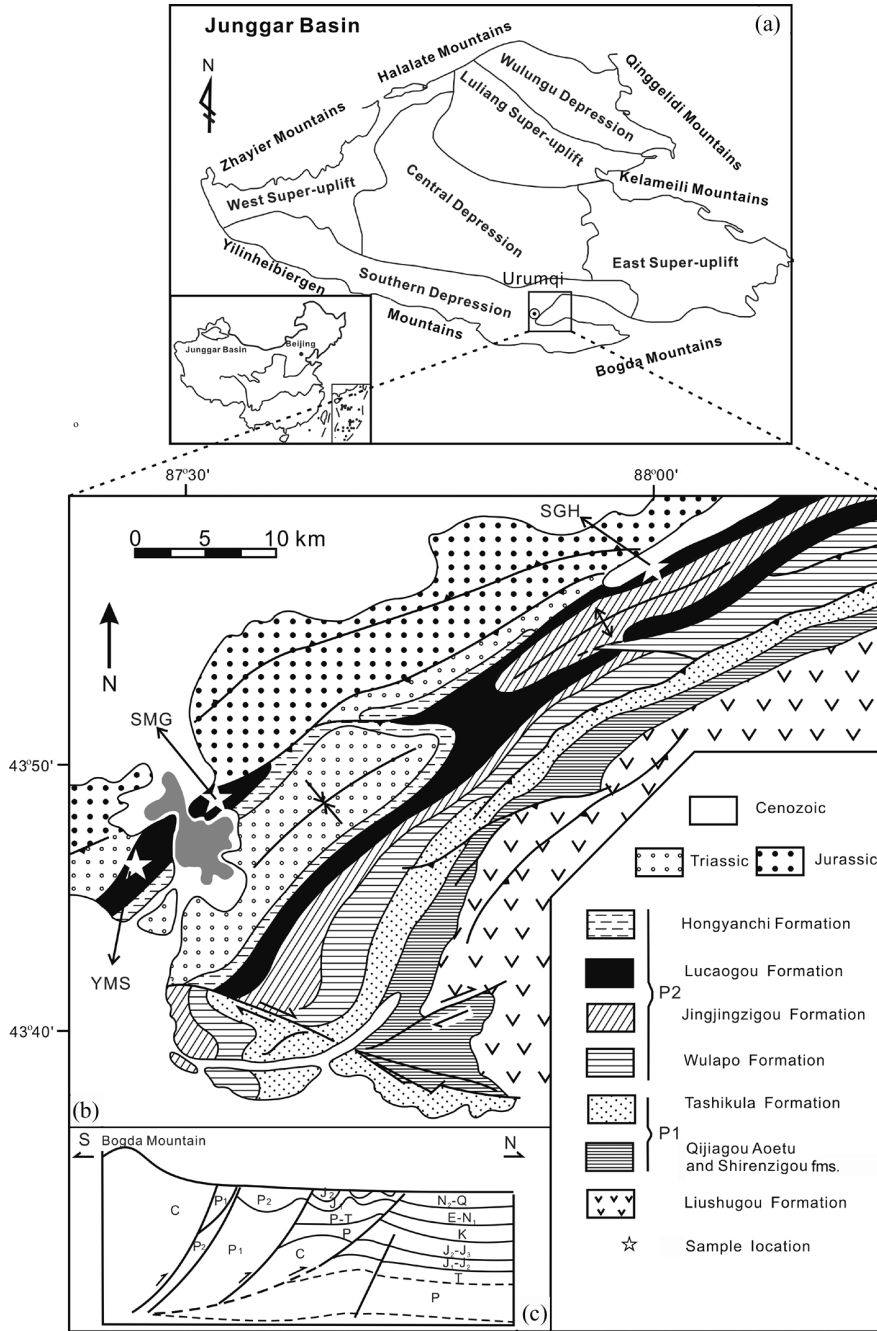


Fig. 1. Generalized map showing the location of the study area: (a) simplified geologic map, (b) cross-section from the western Bogda Mountain showing the location of the measured Yaomoshan, Shuimogou and Sangonghe sections, SE Junggar Basin, modified after [17, 18], (c) cross-section from the northern Bogda Mountain near the Sangonghe River, simplified from [19]. (Abbreviations: SGH – Sangonghe; SMG – Shuimogou; YMS – Yaomoshan; fms. – formations.)

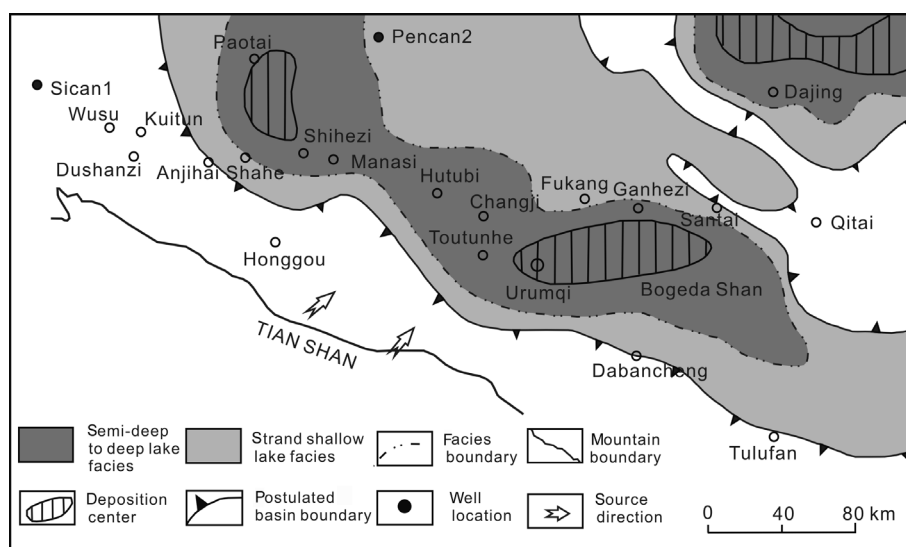


Fig. 2. Sketchy map illustrating the depositional environment in the southern area of the Junggar Basin during the accumulation of the Upper Permian Lucaogou Formation, SE Junggar Basin, modified after [10, 24].

lake environment during the period of the highstand systems tract. The latter segment chiefly consists of grey black thick-layered oil shale interbedded with disseminated dolomitic limestone concretions in the lower part and gradually changing to a submillimeter-scale oil shale layer interbedded with several thin layers of dolomitic limestone in the upper part [9, 10, 14]. Carbonate concretion precipitation in the lower part of segment 3 may be diagenetic and displace the primary structure. This distribution may reflect the corresponding bedrock controlled water column chemistry of alkali. However, the interbedded thin-layered dolomitic limestone in the upper part of the segment may have recorded the climate changes from unfavourable to appropriately warm for carbonate precipitation. Disseminated pyrite and siderite are common in the third segment of Lucaogou Formation mudstone [9, 10, 14]. The presence of pyrite and siderite crystals large enough to be seen with the naked eye may be due to their diagenetic origin [26, 27]. These minerals are common in the semi-deep to deep lacustrine environment, and are indicative of the redox condition of bottom waters. The Lucaogou Formation contains abundant fossils of freshwater organisms such as *Tianshaniscus longipterus*, *Turfania taoshuyuanensis*, *Anthraconauta pseudophilipsii*, *Anthraconauta ilijinskiensis*, *Darwinula parallela*, *Darwinula ornata* and *Darwinula momitoria* [28–31].

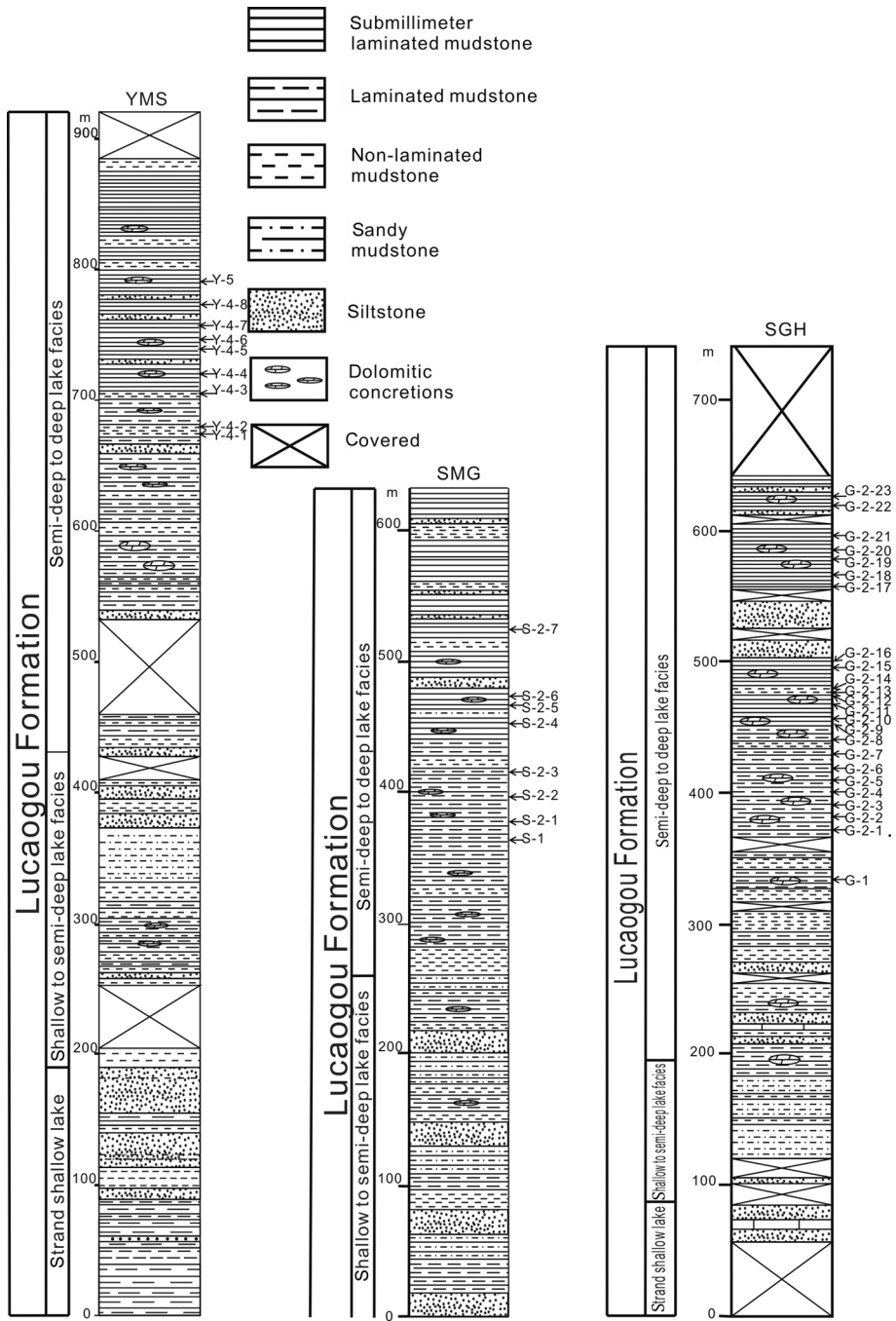


Fig. 3. Lithostratigraphic columnar sections for the three measured sections of the Upper Permian Lucaogou Formation, SE Junggar Basin, modified from [4, 9, 10]. (Abbreviations: YMS – Yamalikeshan, SMG – Shuimogou, SGH – Sangonghe.)

## 2. Material and methods

A total of 41 oil shale samples were collected from the Yamalikeshan (nine samples), Shuimogou (eight samples) and Sangonghe (twenty-four samples) outcrop sections (see Fig. 1b for approximate locations and Fig. 3 for positions on the outcrop section). The samples were labelled as indicated in Table 1. All samples were studied by Rock-Eval pyrolysis/TOC, solvent extraction, fractionation, gas chromatography-mass spectrometry (GC-MS) and total organic carbon isotope analyses. Analyses were conducted in the Key Laboratory of Petroleum Resources Research, Institute of Geology and Geophysics, Chinese Academy of Sciences.

Samples for TOC and organic carbonate isotope ( $\delta^{13}\text{C}_{\text{org}}$ ) analyses were decarbonated with 5% HCl, washed with distilled water to neutralize pH and dried in an oven at 50 °C for 24 h. TOC analyses were conducted on the LECO CS-344 carbon/sulphur analyser.  $\delta^{13}\text{C}_{\text{org}}$  analyses were performed with the MAT-252 Mass Spectrometer on  $\text{CO}_2$  generated from the organic carbon that was oxidized in a furnace up to 850 °C filled with CuO oxidant. Isotopic measurements had a standard deviation of 0.2‰ allowing for fluctuations higher than 0.5‰. The stable carbon isotope values are reported in customary notation in ‰ relative to the VPDB carbonate standard.

The Rock-Eval pyrolysis was performed on 50 mg crushed rock samples (100 mesh) by using a Delsi Rock-Eval II instrument.

100 g crushed samples were Soxhlet extracted using chloroform continuously for 72 h. The concentrated extracts were separated into saturated hydrocarbons, aromatic hydrocarbons and non-hydrocarbons and eluted successively with *n*-hexane, toluene and chloroform:methanol (98:2), respectively, by using a silica gel-alumina chromatographic column (after precipitation of asphaltenes). The GC-MS analysis of saturated and aromatic hydrocarbons employed an HP 5973 MSD directly interfaced to an HP 6890 gas chromatograph fitted with a fused silica capillary column (30 m × 0.25 mm I.D., 0.25 μm DB-5 coating). The GC oven temperature was increased from 80 (hold time 1 min) to 300 °C (hold time 30 min) at 3 °C/min. Helium was used as the carrier gas. MS was operated in EI mode at the ionization energy of 70 eV, with a source temperature of 230 °C.

**Table 1. TOC and Rock-Eval data and organic isotope compositions for Lucaogou oil shale samples, SE Junggar Basin**

Sample	Section	TOC, %	S <sub>1</sub> , mg HC/g rock	S <sub>2</sub> , mg HC/g rock	S <sub>1</sub> +S <sub>2</sub> , mg HC/g rock	HI, mg HC/g TOC	OI, mg CO <sub>2</sub> /g TOC	T <sub>max</sub> , °C	δ <sup>13</sup> C <sub>org</sub> , ‰
Y-5	YMS	35.60	1.82	214.48	216.30	602	1	460	-32.2
Y-4-8		9.48	0.62	38.32	38.94	404	26	437	-28.6
Y-4-7		12.50	0.80	55.26	56.06	442	37	437	-31.0
Y-4-6		9.13	0.31	39.26	39.57	430	42	438	-29.8
Y-4-5		14.30	0.72	63.96	64.68	447	36	440	-29.6
Y-4-4		11.70	0.62	45.54	46.16	389	34	434	-27.6
Y-4-3		2.04	0.09	1.83	1.92	89	76	436	-24.8
Y-4-2		8.65	0.59	32.56	33.15	376	22	432	-27.8
Y-4-1		1.45	0.17	1.73	1.90	119	52	439	-26.4
S-2-7	SMG	12.70	1.21	66.56	67.77	524	5	440	-28.5
S-2-6		4.16	1.45	17.36	18.81	417	35	441	-25.7
S-2-5		4.17	1.33	16.92	18.25	405	37	435	-26.6
S-2-4		2.31	0.59	13.04	13.63	564	33	437	-28.8
S-2-3		1.55	2.22	7.96	10.18	513	65	440	-26.9
S-2-2		1.74	2.56	10.85	13.41	621	83	435	-28.3
S-2-1		4.39	1.92	24.31	26.23	553	55	434	-31.8
S-1		2.89	5.91	15.28	21.19	528	32	434	-25.8
G-2-23		SGH	10.70	2.01	70.32	72.33	657	40	444
G-2-22	8.83		0.93	46.04	46.97	521	23	440	-29.7
G-2-21	11.30		1.12	66.96	68.08	592	26	444	-32.6
G-2-20	10.80		1.28	59.80	61.08	553	20	445	-31.1
G-2-19	15.20		2.32	83.16	85.48	547	20	446	-32.2
G-2-18	9.60		0.72	45.20	45.92	470	35	439	-32.2
G-2-17	21.50		1.25	86.88	88.13	404	39	438	-32.2
G-2-16	5.86		0.47	30.34	30.81	517	36	441	-31.0
G-2-15	6.89		0.56	30.46	31.02	442	42	443	-29.8
G-2-14	5.16		0.40	23.60	24.00	457	20	438	-29.2
G-2-13	9.69		0.61	46.56	47.17	480	37	438	-30.3
G-2-12	4.37		0.28	23.96	24.24	548	30	442	-31.8
G-2-11	17.70		1.88	85.24	87.12	481	49	436	-32.0
G-2-10	6.67		0.44	29.64	30.08	444	36	441	-30.1
G-2-9	11.80		1.50	60.34	61.84	511	28	443	-29.2
G-2-8	4.09		0.51	15.35	15.86	375	46	440	-28.3
G-2-7	5.96		0.56	39.52	40.08	663	31	441	-31.2
G-2-6	22.50		2.06	118.12	120.18	524	20	436	-32.0
G-2-5	8.43		0.67	50.34	51.01	597	32	433	-31.1
G-2-4	18.90		0.61	112.24	112.85	593	19	440	-28.7
G-2-3	21.30		1.86	116.25	118.11	546	23	435	-31.5
G-2-2	14.10	1.17	81.28	82.45	576	27	438	-31.1	
G-2-1	18.60	2.90	108.76	111.66	584	26	439	-31.1	
G-1	17.30	1.86	101.96	103.82	589	23	442	-31.3	

Abbreviations: YMS – Yamalikeshan, SMG – Shuimogou, SGH – Sangonghe.

### 3. Results and discussion

#### 3.1. Rock-Eval pyrolysis

Rock-Eval and TOC data of oil shale samples collected from the YMS, SMG and SGH sections are summarized in Table 1. The TOC content ranges of the samples are 1.45–35.60, 1.55–12.70 and 4.09–22.50%, respectively (Fig. 4a), the average TOC values are 8.66 (except for sample Y-5), 4.24 and 11.97%, respectively. So, the TOC values of all the samples remain within the range of 1.45–22.50%, except for one sample (Y-5 from the YMS section containing shale oil and being ignitable) whose TOC value is 35.60%. The total generation potential ( $S_1 + S_2$ ) of YMS, SMG and SGH oil shales varies from 1.90 to 216.30, between 10.18 and 67.77, and from 15.86 to 120.18 mg HC/g rock, respectively. The  $S_1 + S_2$  value of the SGH oil shale is constantly higher, averaging 65.01 mg HC/g rock, compared with the 35.30 mg HC/g rock (without sample Y-5) and 23.68 mg HC/g rock for the YMS and SMG oil shales, respectively (Fig. 4b).

The values of TOC and  $S_1 + S_2$  indicate that Lucaogou oil shales in the study area are rich in organic matter and have a high oil-generating potential, the SGH oil shale having the highest TOC and  $S_1 + S_2$  values.

Oil shales of the three sections have hydrogen index (HI) values of 89–602, 405–621 and 375–663 mg HC/g TOC, averaging respectively 366, 516 and 528 mg HC/g TOC. Their oxygen index (OI) values range from 1 to 76, between 5 and 83, and from 19 to 49 mg  $CO_2$ /g TOC, and average 36, 43 and 30 mg  $CO_2$ /g TOC, respectively (Table 1). Oil shale from the SGH section is characterized by higher hydrogen index values and lower oxygen index values. On plots of HI vs  $T_{max}$  (Fig. 5a, the kerogen type line based on [32]) and plots of HI vs OI (Fig. 5b, the kerogen type line based on [33]), samples from the three sections plot around the Type II boundary, with most of the YMS samples being in the Type II–III area, the SMG samples along the Type II line, and the SGH samples in the Type I–II area. Based on the plot of  $S_2$  vs TOC, the organic matter in all oil shale samples can be classified as Type II<sub>1</sub> kerogen, except for samples Y-4-3 and Y-4-1 whose kerogen is of Type III (Fig. 6, without sample Y-5, the kerogen type line based on [34]).

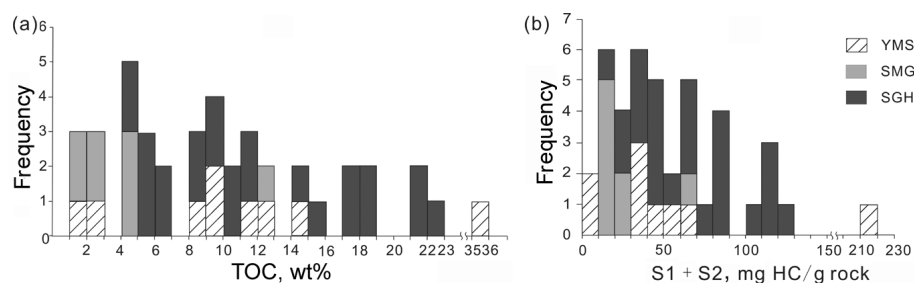


Fig. 4. Cumulative frequency diagrams for TOC (wt%) and  $S_1 + S_2$  (mg HC/g rock) for Lucaogou oil shale samples, SE Junggar Basin. (Abbreviations: YMS – Yamalikeshan, SMG – Shuimogou, SGH – Sangonghe.)

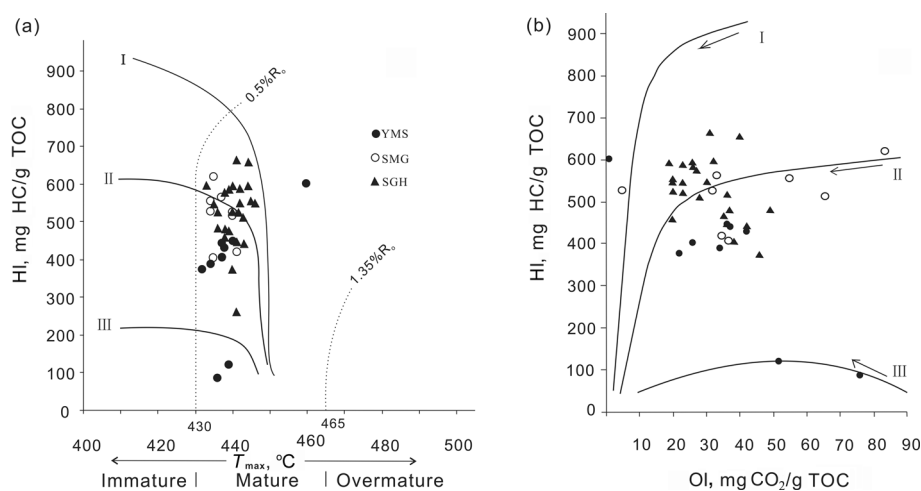


Fig. 5. HI vs  $T_{max}$  distribution (a) and HI vs OI distribution (b) for Lucaogou oil shale samples, SE Junggar Basin. (Abbreviations: YMS – Yamalikeshan, SMG – Shuimogou, SGH – Sangonghe.)

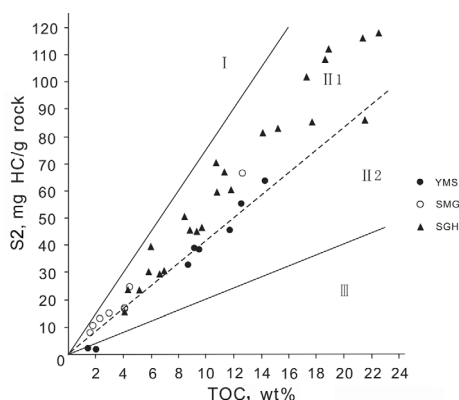


Fig. 6. S2 vs TOC distribution for Lucaogou oil shale samples, SE Junggar Basin. (Abbreviations: YMS – Yamalikeshan, SMG – Shuimogou, SGH – Sangonghe.)

Dembicki [35] observed that when 25% Type III kerogen is mixed with Type I kerogen, the source rock appears to contain Type II kerogen, and when more Type III kerogen is added to the mix, the data could easily be interpreted as a mixture of types II and III [35]. Obviously, the quality of the kerogen of oil shales becomes gradually higher from the YMS section to the SGH section. Therefore, it is more reasonable to define the kerogen type of the three oil shales as a mixture of types I and III, with a higher input of terrestrial organic matter in the YMS oil shale compared with the oil shales of the other two sections. Based on this it may be stated that the oil shales may have been deposited in a single lake with the Sangonghe section as a depocenter which was further away from external sources.

As is clear from the above, there are great differences in TOC and  $S_2$  values among the samples even within the same section, which is usually considered homogeneous. This may be explained by the different organic richness of the samples caused by the different organic input into the sediments due to seasonal changes.

The  $T_{max}$  values which range from 432 to 460, between 434 and 441, and from 433 to 446 °C, and average 437, 437 and 440 °C for the three respective sections (Table 1) suggest that their thermal maturity is immature to mature, early in the oil window (Fig. 5a). This pronouncement is in agreement with the finding of a previous report about Upper Permian oil shales in the southern Junggar Basin with  $R_o$  of 0.54–0.91% [36].

### 3.2. Chloroform extract and its group composition

The chloroform extract (CE) content of all the oil shale samples of the Lucaogou Formation ranged from 0.013 to 0.373% (wt% of rock), being mostly between 0.050 and 0.300%, with an average value of 0.175% (Table 2). The average CE value of the samples was 0.163, 0.117 and 0.191%, respectively, with the highest value occurring in the SGH oil shale and the lowest in the SMG oil shale. The total hydrocarbon (saturated hydrocarbons plus aromatic hydrocarbons) content of the samples was between 52 and 1917 ppm (without sample Y-5) and averaged 700 ppm, the SGH oil shale possessing the highest average value, 788 ppm. The average values for the YMS and SMG oil shales were respectively 569 and 565 ppm. So the yield of soluble organic matter of the samples was relatively high, indicating that the oil shales are good hydrocarbon source rocks, the SGH oil shale being the richest source rock.

The CEs consist of 8.9–47.8% saturates, 2.2–26.2% aromatics, 30.3–85.3% non-hydrocarbons and 1.2–8.9% asphaltenes (wt% of the extract) (Table 2). In general, the ratio of saturated to aromatic hydrocarbons in Type I kerogen is above 3, between 3 and 1 in Type II kerogen, and below 1 in Type III kerogen [37]. For the YMS, SMG and SGH oil shales, this ratio varies between 0.77 and 2.40, from 1.18 to 3.57, and between 1.36 and 4.45, averaging 1.34, 2.22 and 2.70, respectively (Table 2). The ratio increases from the YMS section to the SGH section, which is indicative of the higher quality of kerogen of the SGH oil shale, as also demonstrated by the Rock-Eval data analysis. In view of the above, we can conclude that the kerogen types of oil shales of the three sections are a mixture of types I and III, with the SGH section oil shale having experienced a higher sapropelic parent material input.

**Table 2. Bulk geochemical parameters for Lucaogou oil shale samples, SE Junggar Basin**

Sample	Section	Chloroform extract, %	Saturated HC <sup>a</sup> , %	Aromatic HC <sup>a</sup> , %	Non-HC <sup>a</sup> , %	Asphaltene, %	Total HC <sup>a</sup> , ppm	Saturated HC/aromatic HC
Y-5	YMS	0.314	40.7	26.2	30.9	2.2	2102	1.55
Y-4-8		0.188	24.5	20.6	53.2	1.7	846	1.19
Y-4-7		0.338	14.9	13.5	68.4	3.2	959	1.10
Y-4-6		0.133	18.8	21.7	57.3	2.2	539	0.87
Y-4-5		0.231	9.6	12.5	75.6	2.3	510	0.77
Y-4-4		0.168	18.9	12.9	64.9	3.3	535	1.47
Y-4-3		0.013	25.0	15.3	52.5	7.2	52	1.63
Y-4-2		0.199	23.2	22.0	51.8	3.0	897	1.05
Y-4-1		0.033	45.6	19.0	30.3	5.1	214	2.40
S-2-7	SMG	0.233	31.3	21.9	43.9	2.9	1241	1.43
S-2-6		0.117	29.6	8.3	60.4	1.7	443	3.57
S-2-5		0.064	32.1	12.0	53.7	2.2	282	2.68
S-2-4		0.106	28.9	14.8	49.9	6.4	464	1.95
S-2-3		0.037	41.8	17.5	35.7	5.0	222	2.39
S-2-2		0.097	22.7	15.6	52.8	8.9	371	1.46
S-2-1		0.034	23.5	19.9	50.6	6.0	146	1.18
S-1		0.246	41.4	13.5	43.2	1.9	1349	3.07
G-2-23		SGH	0.373	32.8	7.7	50.7	8.8	1512
G-2-22	0.233		47.0	12.4	38.7	1.9	1385	3.79
G-2-21	0.274		28.4	10.6	58.2	2.8	1067	2.68
G-2-20	0.294		34.5	15.3	47.5	2.7	1464	2.25
G-2-19	0.316		43.9	16.5	38.1	1.6	1911	2.66
G-2-18	0.198		28.6	16.8	52.2	2.4	897	1.70
G-2-17	0.228		12.0	6.5	74.1	7.4	422	1.83
G-2-16	0.105		37.4	12.4	46.1	4.1	525	3.02
G-2-15	0.137		47.8	12.6	36.9	2.7	827	3.82
G-2-14	0.094		35.7	18.9	41.8	3.6	512	1.89
G-2-13	0.134		19.9	14.6	63.1	2.4	461	1.36
G-2-12	0.088		40.1	22.2	34.5	3.2	546	1.81
G-2-11	0.176		9.8	7.2	74.8	8.2	300	1.37
G-2-10	0.096		33.4	16.6	48.1	1.8	481	2.01
G-2-9	0.362		36.9	16.0	45.9	1.2	1917	2.31
G-2-8	0.074		43.6	16.7	37.2	2.5	447	2.61
G-2-7	0.103		15.5	6.4	75.1	3.0	226	2.42
G-2-6	0.191		16.3	7.7	73.3	2.7	458	2.13
G-2-5	0.144		28.0	9.7	60.3	2.0	544	2.88
G-2-4	0.285		10.8	3.0	79.6	6.6	394	3.53
G-2-3	0.187		8.9	2.2	85.3	3.6	208	3.97
G-2-2	0.192	30.2	10.3	58.1	1.4	779	2.93	
G-2-1	0.309	31.5	7.1	60.0	1.4	1193	4.45	
G-1	0.181	18.1	6.0	74.0	1.9	436	3.02	

<sup>a</sup> HC = hydrocarbons. Abbreviations: YMS – Yamalikeshan, SMG – Shuimogou, SGH – Sangonghe.

### 3.3. Molecular composition of organic matter

#### 3.3.1. *n*-Alkanes and isoprenoids

Gas chromatograms of the saturated hydrocarbons isolated from the oil shale samples under study are shown in Figure 7, their parameters are given in Table 3. Generally, *n*-alkanes are in the C<sub>12</sub>–C<sub>35</sub> range, showing a unimodal distribution. The ratio of  $\sum nC_{21}^- / \sum nC_{22}^+$  is used as a relative indicator of terrigenous vs lower-organism organic matter input, but is also sensitive to thermal maturation and biodegradation. Long-chain *n*-alkanes in the range C<sub>10</sub>–C<sub>24</sub> degrade most rapidly due to biological activity. Normal alkanes of greater chain length are more difficult to be consumed by microorganisms. In view of this, the ratio of  $\sum nC_{21}^- / \sum nC_{22}^+$  should decrease due to biodegradation. Since the kerogen of the YMS oil shale is mostly of Type III, suggesting a significant input of land-plant organic matter, the relatively high values of  $\sum nC_{21}^- / \sum nC_{22}^+$  (0.55–2.87) for this oil shale may be the consequence of maturation. In addition, a study demonstrated that certain non-marine algae, e.g., *Scenedesmus quadricauda*, *Tetrahedron sp.*, *Anacystis montana* and *Botryococcus braunii*, produce a significant amount of

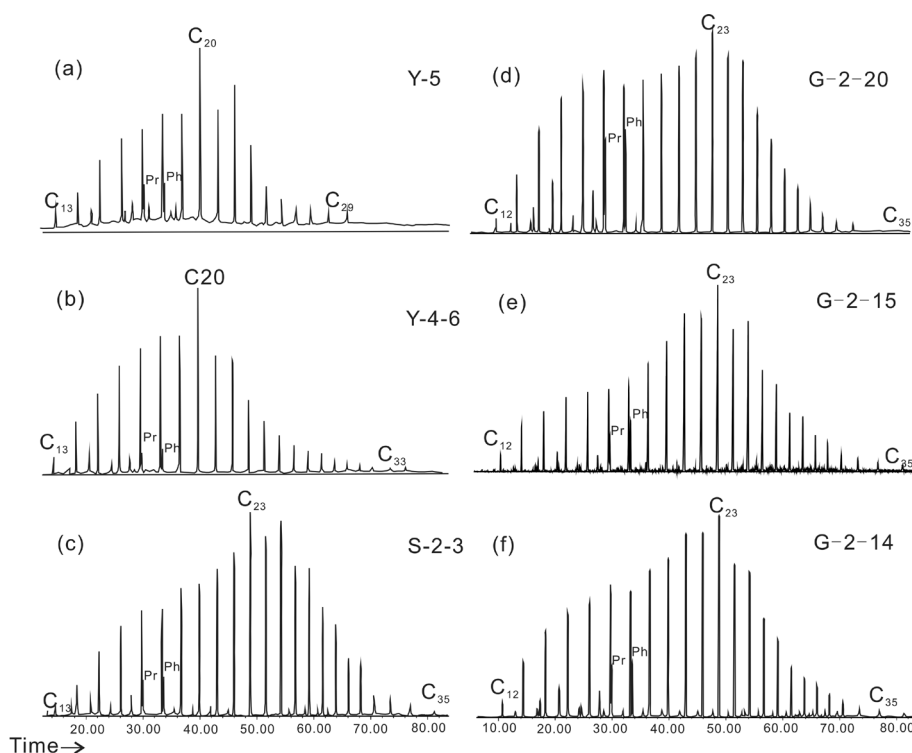


Fig. 7. Representative chromatograms of *n*-alkanes (*m/z* 85) for Lucaogou oil shale samples, SE Junggar Basin.

Table 3. Molecular parameters for the extractable organic matter of Lucaogou oil shale samples, SE Junggar Basin

Sample	Section	C <sub>range</sub>	C <sub>max</sub>	C <sub>21</sub> –/C <sub>22</sub> <sup>+</sup>	OEP	Pr/Ph	Pr/C <sub>17</sub>	Ph/C <sub>18</sub>	Ts/Tm	Gamma index <sup>a</sup>	22S/(22S + 22R) C <sub>31</sub> homohopane	αββ/(αββ + ααα) C <sub>29</sub> sterane	20S/(20S + 20R) C <sub>29</sub> sterane	C <sub>27</sub> sterane, %	C <sub>28</sub> sterane, %	C <sub>29</sub> sterane, %
Y-5	YMS	13-29	20	2.43	0.68	1.04	0.53	0.50	0.47	11	0.59	0.37	0.45	19	33	48
Y-4-8		12-35	20	2.19	0.82	1.31	0.33	0.26	0.43	12	0.58	0.31	0.45	17	34	49
Y-4-7		12-33	17	2.36	1.03	1.10	0.29	0.37	0.36	12	0.59	0.31	0.43	18	33	49
Y-4-6		12-33	20	2.53	0.75	1.36	0.22	0.15	0.40	12	0.60	0.32	0.46	19	34	47
Y-4-5		13-35	20	2.75	0.84	1.36	0.20	0.14	0.36	14	0.61	0.28	0.46	24	33	43
Y-4-4		13-35	21	1.61	1.07	1.35	0.30	0.23	0.38	7	0.60	0.27	0.44	23	31	46
Y-4-3		13-35	17	1.38	1.01	1.52	0.50	0.38	0.27	7	0.60	0.29	0.42	28	29	43
Y-4-2		13-33	17	2.87	1.07	1.42	0.18	0.16	0.36	10	0.60	0.28	0.47	25	29	46
Y-4-1		13-35	25	0.55	1.03	1.33	0.77	0.51	0.75	7	0.61	0.35	0.46	28	26	46
S-2-7	SMG	12-35	17	3.43	1.10	1.31	0.17	0.16	0.38	5	0.59	0.33	0.48	23	27	50
S-2-6		12-37	21	1.14	1.06	1.31	0.75	0.57	0.26	10	0.59	0.26	0.33	21	34	45
S-2-5		12-35	21	0.99	1.02	1.16	0.85	0.76	0.24	9	0.58	0.29	0.35	22	36	42
S-2-4		13-35	27	0.23	1.09	1.21	1.55	1.22	0.25	9	0.59	0.27	0.35	20	32	48
S-2-3		13-35	23	0.59	1.14	1.02	0.39	0.38	0.31	5	0.59	0.26	0.39	19	28	53
S-2-2		12-35	23	0.61	1.11	1.23	0.61	0.50	0.25	16	0.59	0.23	0.32	30	22	48
S-2-1		12-35	22	1.02	0.90	1.56	0.36	0.25	0.25	10	0.60	0.27	0.34	17	35	48
S-1		12-37	23	0.45	1.16	1.21	0.67	0.58	0.25	8	0.60	0.27	0.38	16	33	51
G-2-23		12-35	23	0.48	1.12	0.93	1.12	1.29	0.36	17	0.59	0.17	0.27	16	34	50
G-2-22		12-35	23	0.75	1.13	1.38	1.63	1.18	0.30	4	0.58	0.17	0.27	22	31	47
G-2-21		12-35	23	0.85	1.20	1.16	0.91	0.74	0.30	3	0.58	0.21	0.31	24	31	45

(Continuation of Table 3)

Sample	Section	C <sub>range</sub>	C <sub>max</sub>	C <sub>21</sub> -/C <sub>22</sub> <sup>+</sup>	OEP	Pr/Ph	Pr/C <sub>17</sub>	Ph/C <sub>18</sub>	Ts/Tm	Gamma index <sup>a</sup>	22S/(22S + 22R) C <sub>31</sub> homohopane	αββ/(αββ + ααα) C <sub>29</sub> sterane	20S/(20S + 20R) C <sub>29</sub> sterane	C <sub>27</sub> sterane, %	C <sub>28</sub> sterane, %	C <sub>29</sub> sterane, %
G-2-20	SGH	12-35	23	1.12	1.07	0.87	0.77	0.74	0.32	6	0.59	0.24	0.36	25	26	49
G-2-19		12-35	23	1.18	1.06	1.19	0.75	0.69	0.29	3	0.59	0.23	0.35	20	29	51
G-2-18		12-35	23	0.90	1.07	1.23	0.66	0.58	0.32	5	0.58	0.22	0.36	20	37	43
G-2-17		12-35	22	0.95	0.98	1.21	0.63	0.49	0.24	4	0.59	0.19	0.35	21	33	45
G-2-16		12-35	23	1.12	1.18	1.44	0.45	0.32	0.30	2	0.59	0.21	0.33	20	37	43
G-2-15		12-35	23	0.81	1.20	0.92	0.57	0.63	0.33	3	0.60	0.23	0.33	19	36	45
G-2-14		12-35	23	1.10	1.14	0.84	0.50	0.47	0.25	2	0.59	0.21	0.35	18	38	44
G-2-13		12-35	17	1.60	1.09	1.36	0.85	0.69	0.25	4	0.60	0.23	0.37	25	30	45
G-2-12		12-35	23	0.70	1.09	1.25	0.92	0.82	0.30	5	0.58	0.22	0.36	15	28	57
G-2-11		12-35	22	1.18	0.89	1.43	0.77	0.59	0.28	6	0.58	0.21	0.39	22	34	44
G-2-10		12-35	23	0.86	1.11	1.34	1.49	1.02	0.22	3	0.59	0.19	0.34	16	32	52
G-2-9		12-35	23	0.82	1.03	1.00	1.32	1.38	0.36	11	0.59	0.24	0.39	27	29	44
G-2-8		12-37	23	0.70	1.10	1.27	0.57	0.45	0.38	9	0.60	0.23	0.39	17	37	46
G-2-7		12-35	20	1.54	0.93	1.31	0.91	0.65	0.25	11	0.58	0.26	0.36	24	33	44
G-2-6		12-33	20	1.57	0.97	1.20	0.73	0.67	0.22	14	0.58	0.22	0.38	31	37	32
G-2-5		12-37	22	0.94	0.98	1.12	0.50	0.42	0.33	14	0.59	0.26	0.41	20	36	45
G-2-4		13-33	20	2.62	0.77	1.45	0.14	0.07	0.30	6	0.59	0.23	0.39	16	46	39
G-2-3		13-37	20	1.73	0.84	1.31	0.17	0.10	0.42	6	0.58	0.25	0.41	19	45	36
G-2-2		12-37	21	1.25	1.00	1.47	0.97	0.62	0.33	25	0.60	0.26	0.43	25	31	44
G-2-1		12-35	21	0.87	1.04	1.45	0.68	0.39	0.29	22	0.59	0.24	0.38	13	31	56
G-1	12-35	17	2.06	0.98	1.75	0.86	0.54	0.06	14	0.59	0.18	0.34	10	38	52	

<sup>a</sup> Gamma index = [Gammacerane/C<sub>30</sub>17α(H),21β(H)-hopane]\*100. OEP – odd-to-even preference ratio of *n*-alkanes. Abbreviations: YMS – Yamalikeshan, SMG – Shuimogou, SGH – Sangonghe.

both medium- and high-molecular-weight paraffins [38]. Therefore, the simultaneous presence of the above algae in the SMG and SGH oil shale samples may explain their higher ratio of  $\sum nC_{21}^-/\sum nC_{22}^+$ .

The values of the odd-to-even preference ratio of n-alkanes (OEP) for samples Y-5, Y-4-8, Y-4-6 and Y-4-5 are 0.68, 0.82, 0.75 and 0.84, respectively. Of n-alkanes, n-C<sub>20</sub> turns out to be the most abundant, showing the predominance of even-numbered species, especially those ranging from n-C<sub>18</sub> to n-C<sub>22</sub>, which is indicative of microbial activities in sediments [39]. In the extracts from the SMG and SGH oil shales (Fig. 7), mainly n-C<sub>20</sub> to n-C<sub>23</sub> alkanes prevail, implying the contribution of non-marine brackish water algae or aquatic macrophytes [37, 40–43]. However, the ratio of  $\sum nC_{21}^-/\sum nC_{22}^+$  for most of the SMG oil shale samples is lower than 1, suggesting the origin of lipids from higher plants [44–47]. Therefore, the oil shale of the SMG section may represent a mixed-source depositional environment including higher terrestrial plants, aquatic macrophytes and algae. In contrast, the ratio of  $\sum nC_{21}^-/\sum nC_{22}^+$  for most of the SGH oil shale samples is higher than 1, pointing to the provenance dominated by lower organisms.

In most samples, pristane (Pr) is more abundant than phytane (Ph), the Pr/Ph ratio ranging from 0.84 to 1.75 (Fig. 7, Table 3). On the Pr/nC<sub>17</sub> vs Ph/nC<sub>18</sub> plot (Fig. 8), the samples mostly lie within the zone of mixed organic matter sources and transitional environments, near the reducing zone. This indicates a weakly oxic to reducing transitional depositional

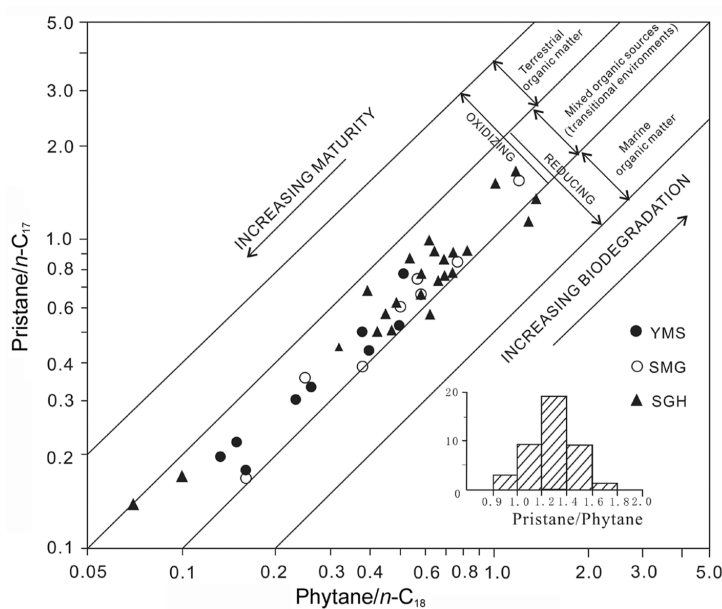


Fig. 8. Plot of Pr/n-C<sub>17</sub> vs Ph/n-C<sub>18</sub> for Lucaogou oil shale samples, SE Junggar Basin. (Abbreviations: YMS – Yamalikeshan, SMG – Shuimogou, SGH – Sangonghe.)

environment for the oil shales under study [48]. Several SGH oil shale samples plot in the reducing zone in Figure 8, referring to the lower organisms input in a reducing environment.

### 3.3.2. Terpanes

The  $m/z$  191 chromatograms of terpanes determined by GC-MS are shown in Figure 9, the homohopane parameters of the studied oil shale samples are reported in Table 3.  $C_{31}$  is the dominant homohopane. The homohopanes distribution exhibits a decrease from  $C_{31}$  to  $C_{35}$  in all the samples (Fig. 9).  $C_{34}$  and  $C_{35}$  homohopanes occur only in low quantities or cannot be detected in the extracts, suggesting a fresh-water non-marine depositional environment [49].

Gammacerane was also present in all samples, exhibiting a characteristic peak. The gammacerane index (gammacerane/ $C_{30}\alpha\beta$ -hopane) varies from 7 to 14, between 5 and 16, and from 2 to 25% (Table 3) for the YMS, SMG, and SGH oil shales, respectively. The presence of gammacerane indicates a stratified water column during source rock sedimentation in marine and non-marine environments, commonly associated with hypersalinity at depth [40, 49–52]. Concentrations of gammacerane are not significant in the oil shales of the studied sections, indicating brackish water depositional conditions.

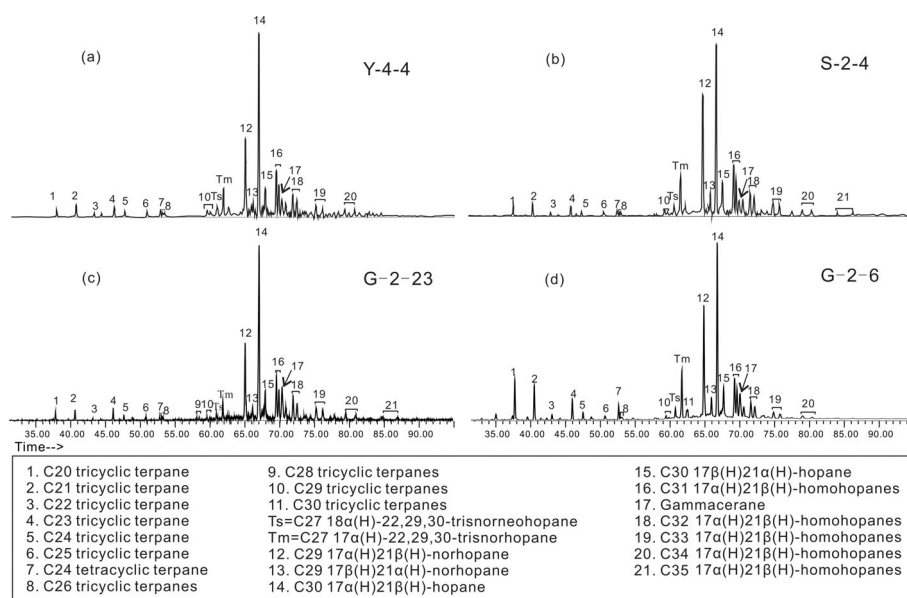


Fig. 9. Representative chromatograms of terpanes ( $m/z$  191) for Lucaogou oil shale samples, SE Junggar Basin.

The 22S/(22S + 22R) ratio for C<sub>31</sub> homohopane increases with thermal maturity (0–0.6) and reaches the equilibrium value at 0.58–0.62 [53]. After reaching equilibrium at the early oil-generative stage, no further maturity information is available because the 22S/(22S + 22R) ratio remains constant [49, 54]. For YMS, SMG and SGH oil shale samples the ratio ranges from 0.58 to 0.61, between 0.58 and 0.60, and from 0.58 to 0.60, respectively, having attained the so-called “equilibrium value”. This indicates that the samples have reached or surpassed the early phase of oil generation (vitrinite reflectance ca 0.5%).

During maturation, C<sub>27</sub> 17 $\alpha$ -trisorhopane (Tm) is less stable than C<sub>27</sub> 18 $\alpha$ -trisorhopane (Ts) and the Ts/Tm ratio increases with maturity [55]. This ratio is also dependent on sedimentary facies and depositional environment. Redox potential can have a higher effect on the relative amount of Ts and Tm than maturity, with the Ts/Tm ratio smaller than 1 even in highly mature anoxic sediments. With the similar thermal maturity, sediments deposited in the anoxic environment tend to have lower Ts/Tm ratio than those deposited in the oxidizing environment [40, 56]. In the oil shale samples analysed, the Ts/Tm ratio values (0.27–0.75, 0.24–0.38 and 0.06–0.42 for the YMS, SMG and SGH sections, respectively) are not consistent with those of the other maturity parameters, such as  $T_{max}$  and the  $\alpha\beta$ C<sub>31</sub> 22S/(22S + 22R) ratio. These relatively low values of Ts/Tm in the oil shale samples of the three sections may indicate anoxic depositional conditions, and, probably due to the deeper water, a more reducing environment for the SGH section whose Ts/Tm ratio is lower than those for the other two sections.

Established from organic geochemical data the water depth distribution agrees well with the assumption about the area’s paleogeography put forward by Peng et al. [13], Carroll et al. [16] and Wartes et al. [20]. Based on the correlation between the lithostratigraphic cross sections of Upper Permian rocks, the Junggar and Turpan-Hami basins were supposed to have been occupied by a single large lake that was comparable in size to the modern Caspian Sea [16, 20]. According to the well connecting profile and sequence stratigraphic data, Peng et al. [13] suggested that the YMS, SMG and SGH sections were occupied by a single large lake during the deposition period of the Lucaogou Formation, with the Sangonghe section as a depocenter having the maximum water depth and being further away from the external source. In the Lucaogou Formation, the sediments thickness was the greatest, up to 1000 m, in the SGH section, which then decreased significantly from the east to the west, reaching below 400 m in the YMS section [13].

### 3.3.3. Steranes

The distribution of regular C<sub>27</sub>, C<sub>28</sub> and C<sub>29</sub> steranes can reflect the source of organic matter in sediments. Previous studies have shown that the enhanced amount of C<sub>27</sub> steranes may be derived from marine phytoplankton, the high concentration of C<sub>28</sub> steranes may be related to lacustrine algae and the

increased amount of  $C_{29}$  steranes may indicate the contribution from higher land plants [40, 48, 57]. In addition, it has been proposed that numerous microorganisms such as primitive algae [58], cyanobacteria [59], diatoms and freshwater eustigmatophytes [43] could be alternative sources for  $C_{29}$  steranes.

Most of the oil shale samples under study have a similar distribution of  $C_{27}$ ,  $C_{28}$  and  $C_{29}$  steranes –  $C_{29} > C_{28} > C_{27}$  (Figs. 10 and 11, and Table 3), which is a sign of their similar organic matter type and depositional paleo-environment. The slightly higher amount of  $C_{29}$  steranes (32–57%) does not necessarily suggest the dominance of higher plant organic matter input, since the compounds may also originate from other sources. In all of the studied oil shale samples, the concentrations of  $C_{28}$  steranes (22–46%) and  $C_{29}$  steranes (32–57%) are close, which is indicative of a high contribution of lacustrine algae. The  $C_{28}/C_{29}$  sterane ratio of SGH oil shale samples is higher than those of YMS and SMG oil shale samples, signifying a higher input of lacustrine algae in the SGH section compared to the other two.

For  $C_{29}$  steranes the isomerization ratios  $S/(S + R)$  and  $\alpha\beta\beta/(\alpha\alpha\alpha + \alpha\beta\beta)$  are the two most commonly used sterane maturity parameters. Both increase with maturity and reach equilibrium values of approximately 0.55 (vitrinite reflectance about 0.8–0.9%) and ca 0.70 (vitrinite reflectance about 0.91–1.0%) around peak oil generation, respectively [49, 54, 60]. In YMS, SMG and SGH oil shale samples, the above ratios are lower than the equilibrium values (Table 3, Fig. 12), suggesting that oil shales of the three sections have not reached the thermal maturity level of the late stage of oil generation. These ratios also show that the SMG and SGH oil shale samples are slightly less mature than those of the YMS section (Fig. 12), which is consistent with the values of  $\sum nC_{21}^-/\sum nC_{22}^+$ .

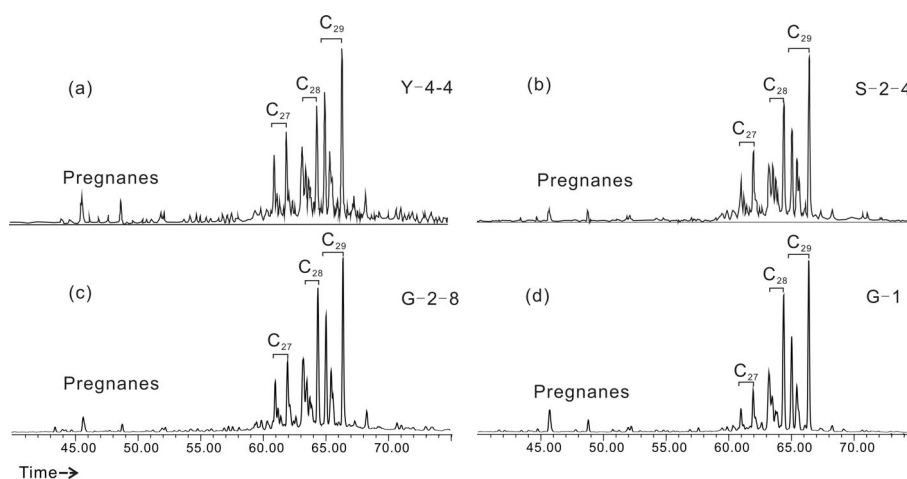


Fig. 10. Representative chromatograms of steranes ( $m/z$  217) for Lucaogou oil shale samples, SE Junggar Basin.

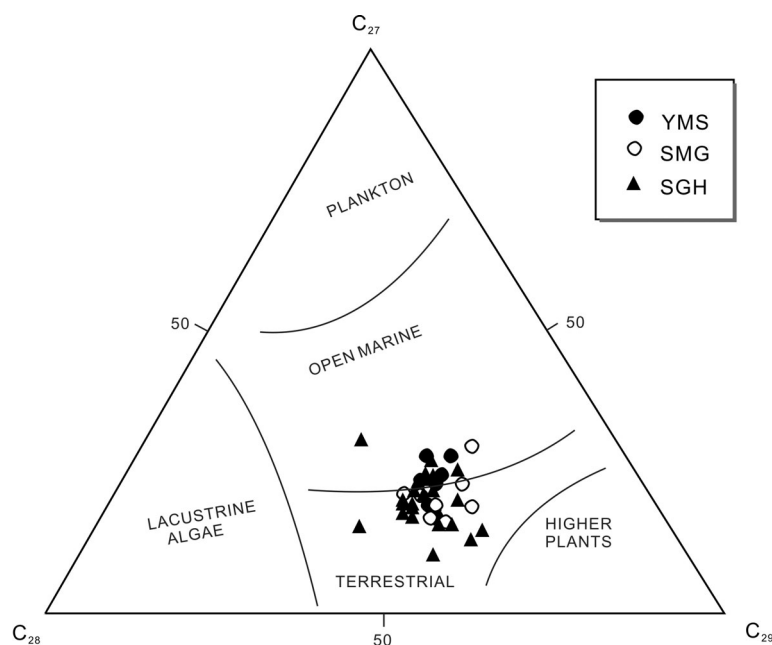


Fig. 11. Ternary diagrams of  $C_{27}$ ,  $C_{28}$  and  $C_{29}$  sterane compositions showing source rock environments for Lucaogou oil shale samples, SE Junggar Basin (the classification line based on [48]). (Abbreviations: YMS – Yamalikeshan, SMG – Shuimogou, SGH – Sangonghe.)

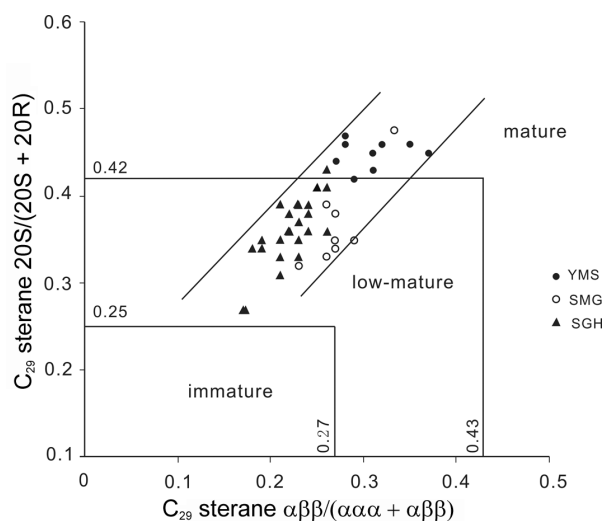


Fig. 12. Cross-plot of  $C_{29}$  sterane  $20S/(20S + 20R)$  ratios vs  $\alpha\beta/(\alpha\alpha + \alpha\beta)$  ratios for Lucaogou oil shale samples, SE Junggar Basin. (Abbreviations: YMS – Yamalikeshan, SMG – Shuimogou, SGH – Sangonghe.)

### 3.3.4. Oxygenated compounds

Of oxygenated compounds, ketones, aldehydes and fatty acid methyl esters (FAMES) were detected in the studied samples. *n*-Alkanones were found in all samples. Samples Y-4-6 and Y-4-5 from the YMS section contained *n*-aldehydes, with the carbon number distribution of C<sub>12</sub>–C<sub>27</sub> and C<sub>12</sub>–C<sub>24</sub>, both maximized at C<sub>21</sub> (Fig. 13). There are two possible sources for these *n*-aldehydes. One is the microbial alteration of other compounds, such as *n*-alkanes, in oil shale. In this case, the distribution of aldehydes is similar to that of *n*-alkanes and ketones [61, 62]. Another possible source is the living organisms growing in or around the lake. In this case, the *n*-aldehydes in the sediments are dominated by the C<sub>22</sub>–C<sub>30</sub> even-carbon-numbered ones. To the best of our knowledge, the supporting studies in this case are all focused on contemporary lake sediments [63, 64]. This may indicate that the *n*-aldehydes from living organisms cannot be preserved after long geological evolution.

The distribution pattern of aldehydes detected in samples Y-4-6 and Y-4-5 is similar to those of alkanes and ketone assemblages (Fig. 13). Based on the

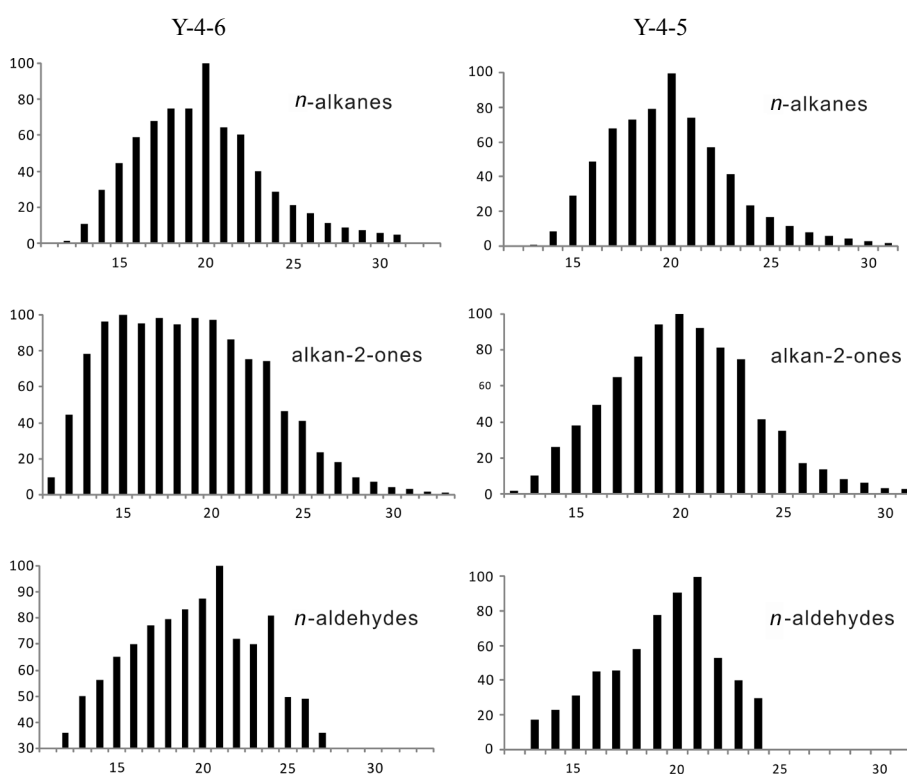


Fig. 13. Carbon number distribution of *n*-alkanes, ketones (alkan-2-ones) and *n*-aldehydes in oil shale samples Y-4-6 and Y-4-5 from the Yamalikeshan section, Lucaogou Formation, SE Junggar Basin.

above discussion, it is suggested that the *n*-aldehydes in the oil shale samples from the YMS section may have been derived from other compounds, such as *n*-alkanes, as a result of their microbial diagenesis.

A prominent suite of FAMES, C<sub>12</sub>–C<sub>30</sub> or C<sub>12</sub>–C<sub>26</sub>, was identified in samples Y-4-2 and Y-4-1 (Fig. 14). Since the solvent used in the Soxhlet extraction is chloroform, the FAMES detected in the extracts cannot be the derivatives of fatty acids liberated from the sediments. The distribution of these esters in both the samples maximized at C<sub>16</sub>, with even-numbered species predominating. Studies of FAMES in geological structures are rare and there are none regarding their occurrence in organisms. Severely alkaline-neutral environments are needed for the existence of FAMES in geological structures [65, 66]. Naturally occurring FAMES are considered to originate from higher plant leaf waxes and suberin [67]. Therefore, the occurrence of FAMES in the two samples may indicate an alkaline-neutral depositional environment. Furthermore, the kerogen type of sample Y-4-1 is III, unlike the other YMS oil shale samples whose kerogen type is a mixture of types I and III. Thus, the occurrence of FAMES may also be related to the higher plant input.

In addition, it is worth noting that none of the samples contained aldehydes and FAMES at the same time. Since aldehydes are very easily oxidized and generate carboxylic acids, their occurrence in the oil shale formation may reflect a reducing lacustrine depositional environment. In contrast, FAMES are very easily reduced and generate alcohols [68]. Therefore, their presence in two YMS oil shale samples may mirror an oxidizing depositional environment. This might explain why aldehydes and FAMES

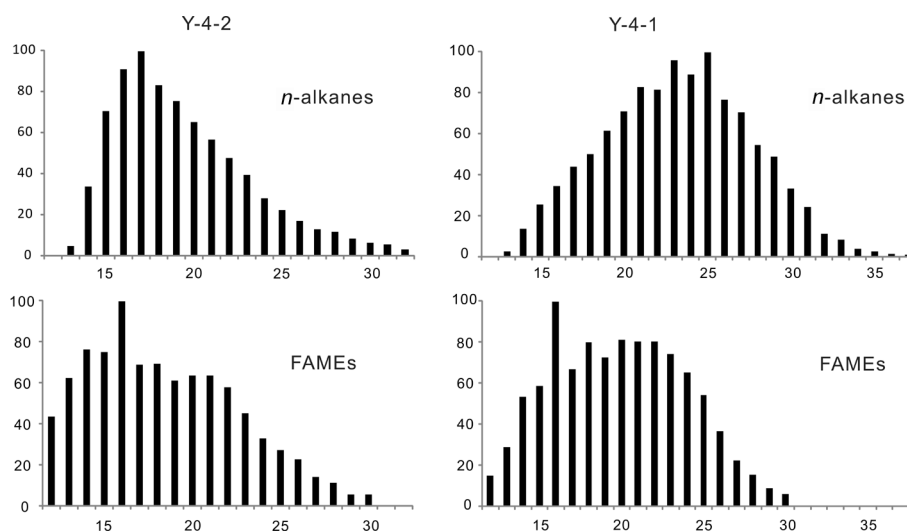


Fig. 14. Carbon number distribution of *n*-alkanes and FAMES in oil shale samples Y-4-2 and Y-4-1 from the Yamalikeshan section, Lucaogou Formation, SE Junggar Basin. (Abbreviation: FAMES – fatty acid methyl esters.)

cannot coexist. The depositional environment changes of the YMS section from oxidizing to anoxic conditions may have been caused by lake level changes. If this was the case, then samples Y-4-6 and Y-4-5 were deposited during the low-lake-level period and samples Y-4-2 and Y-4-1 during the high-lake-level period. The lake level change may have also led to the change of the distance from external sources like higher plants, which in turn accounts for the kerogen type difference between the oil shale samples studied.

### 3.4. Organic carbon isotope

The total organic carbon isotope ( $\delta^{13}\text{C}_{\text{org}}$ ) value is an important proxy for tracing biological sources and palaeoenvironment in lakes. For the samples of the YMS section the  $\delta^{13}\text{C}_{\text{org}}$  values varied from  $-32.2$  to  $-24.8\text{‰}$ , with an average value of  $-28.6\text{‰}$ . The respective figures for the samples from the SMG section ranged between  $-31.8$  and  $-25.7\text{‰}$ , with an average value of  $-27.8\text{‰}$ , and for the samples from the SGH section from  $-33.2$  to  $-29.2\text{‰}$ , averaging  $-30.9\text{‰}$ .

Based on their photosynthetic processes, terrestrial plants are classified into two types:  $\text{C}_3$  and  $\text{C}_4$ . The  $\delta^{13}\text{C}_{\text{org}}$  values of  $\text{C}_3$  plants range from  $-34.0$  to  $-22.0\text{‰}$ , while  $\text{C}_4$  plants have  $\delta^{13}\text{C}_{\text{org}}$  values varying from  $-14.0$  to  $-10.0\text{‰}$ . The great carbon isotopic value difference between terrestrial  $\text{C}_3$  and  $\text{C}_4$  plants is caused by the different types of photosynthesis [69–72]. In addition, aquatic organisms have higher negative  $\delta^{13}\text{C}_{\text{org}}$  values than higher terrestrial plants, and deep water plants have higher negative  $\delta^{13}\text{C}_{\text{org}}$  values than shallow water plants [72, 73].

Based on the above discussion, the  $\delta^{13}\text{C}_{\text{org}}$  values indicate that higher terrestrial plants are dominated by  $\text{C}_3$  plants, suggesting a cool and humid palaeoclimate. This agrees with the evidence of Upper Permian flora which matches with a cool, temperate climate [4, 74–77]. In general, the negative  $\delta^{13}\text{C}_{\text{org}}$  values of the SGH oil shale are higher than those of oil shales of the other two sections (Table 1, Fig. 15). As seen from Figure 15, there is a

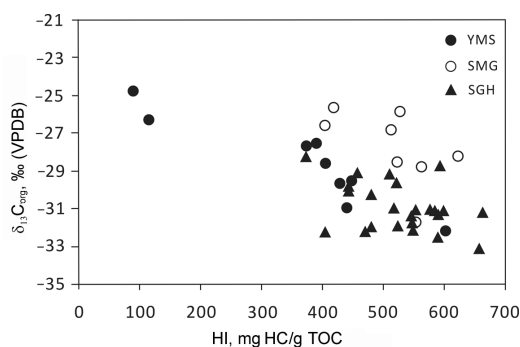


Fig. 15.  $\delta^{13}\text{C}_{\text{org}}$  vs HI plot for Lucaogou oil shale samples, SE Junggar Basin. (VPDB – carbonate standard name of the stable carbon isotope. Abbreviations: YMS – Yamalikeshan, SMG – Shuimogou, SGH – Sangonghe.)

negative correlation between the  $\delta^{13}\text{C}_{\text{org}}$  and HI values of oil shale samples. Therefore, we suggest that the higher negative  $\delta^{13}\text{C}_{\text{org}}$  values of the SGH oil shale compared to those of the YMS and SMG oil shales are the consequence of a higher algal material input, indicating that during the sedimentation period of the Lucaogou Formation the lake water was deeper in the SGH section.

#### 4. Conclusions

1. Oil shales from the Yamalikeshan, Shuimogou and Sangonghe sections of the Lucaogou Formation in the southeastern Junggar Basin, Northeast China are rich in organic matter and have a high hydrocarbon generation potential, as suggested by bulk Rock-Eval and chloroform extract analyses. The different organic content of the samples studied implies that the Sangonghe oil shale has the highest TOC,  $S_1 + S_2$  and chloroform extract values and Sangonghe is the richest hydrocarbon source rock section as established in this study.
2. The kerogen type of Lucaogou Formation oil shales in the study area is a mixture of types I and III, the Yamalikeshan oil shale having enjoyed a relatively high contribution of terrestrial organic matter and the Sangonghe oil shale a higher algal material input, as indicated by Rock-Eval data, chloroform extract analyses, and the normal sterane distribution and organic carbon isotopic data. The kerogen type of oil shales gradually changes from Type III to Type I from the Yamalikeshan section to the Sangonghe section, along the southwest-northeast direction through the foothill of Bogda Mountain. Based on this it appears that the oil shales may have been deposited in a single lake with the Sangonghe section as a depocenter, which was further away from external sources, while the Yamalikeshan section area was closest to the lake shore.
3.  $T_{\text{max}}$  values and hopane isomerisation ratios indicate that the Lucaogou Formation oil shales are low mature to mature, in the early oil window, corresponding to the vitrinite reflectance of 0.54–0.91% reported in the literature. Sterane isomerisation ratios suggest that the oil shale of the Yamalikeshan section is slightly more mature than those of the other two sections.
4. The oil shales analysed in this study were deposited in semi-deep to deep lacustrine environments with fresh to brackish water, under mild anoxic conditions of a cool, humid paleoclimate, as indicated by the plots of  $\text{Pr}/n\text{C}_{17}$  vs  $\text{Ph}/n\text{C}_{18}$ , the values of  $T_s/T_m$  and the organic carbon isotope composition. Some layers were partly subjected to microbial modification, as suggested by the  $n$ -alkane distribution. The Sangonghe section suggested a more reducing, higher salinity and deeper depositional environment and had a more significant aquatic lower organism input compared with the other two sections.

5. In samples Y-4-6 and Y-4-5 from the Yamalikeshan section, ketones and aldehydes were present, showing a similar distribution as *n*-alkanes, which suggests that aldehydes may be the product of the microbial oxidation of *n*-alkanes or other lipids. In samples Y-4-2 and Y-4-1 from the same section, ketones and fatty acid methyl esters occurred, indicating an alkaline-neutral depositional environment during the corresponding deposition intervals. However, no sample contained ketones, aldehydes and fatty acid methyl esters simultaneously, due to the fact that the latter two need a reducing and oxidizing environment respectively to be preserved. This unique occurrence of aldehydes and fatty acid methyl esters is indicative of the varying depositional environment of the Yamalikeshan section.

### Acknowledgements

We would like to thank the anonymous reviewers for giving useful comments on the paper. This research was supported by the Chinese Academy of Sciences Key Project (Grant No. XDB10030404), the Major State Basin Research Development Program of China (No. 2012CB214701), the Chinese Academy of Sciences Key Project (Grant No. XDB03020405), the National Natural Science Foundation of China (Grant Nos. 41172169, 41272147, 40672123), the Western Light Joint Scholars Project, and the Key Laboratory Project of Gansu Province (Grant No. 1309RTSA041).

### REFERENCES

1. Hu, H. *Investigation Report of Oil Shale in Northern Bogda Mountain*. Xinjiang Geological Survey, 1955 (in Chinese).
2. Graham, S. A., Brassell, S., Carroll, A. R., Xiao, X., Demaison, G., Mcknight, C. L., Liang, Y., Chu, J., Hendrix, M. S. Characteristics of selected petroleum source rocks, Xianjiang Uygur Autonomous Region, Northwest China. *AAPG Bull.*, 1990, **74**(4), 493–512.
3. Demaison, G., Huizinga, B. J. Genetic classification of petroleum systems. *AAPG Bull.*, 1991, **75**(10), 1626–1643.
4. Carroll, A. R., Brassell, S. C., Graham, S. A. Upper Permian Lacustrine oil shales, southern Junggar Basin, Northwest China. *AAPG Bull.*, 1992, **76**(12), 1874–1902.
5. Li, J. *The Study on Geochemical Characteristics of Lucaogou Formation Oil Shale at the Northern Foot of Bogda Mountain*. China University of Geosciences for Doctoral Degree, 2009, 17–31 (in Chinese with English abstract).
6. Tao, S., Wang, Y., Tang, D., Xu, H., Zhang, B., He, W., Liu, C. Composition of the organic constituents of Dahuangshan oil shale at the northern foot of Bogda Mountain, China. *Oil Shale*, 2012, **29**(2), 115–127.
7. Wang, D., Tang, D., Gou, M., Wang, F., Tao, S., Gao, G. Oil-shale geology of Lucaogou Formation in Fukang area on southern margin of Junggar Basin.

- China Petroleum Exploration*, 2007, **12**(6), 18–22, 71–72 (in Chinese with English abstract).
8. Wang, D., Xu, H., Li, J., Tao, S., Zhou, C., Gao, G. Analysis on the oil shale geochemical characteristics and sedimentary environments of Lucaogou Formation in Dahuangshan area. *Inner Mongolia Petrochemical Industry*, 2008, **34**(3), 62–65 (in Chinese with English abstract).
  9. Li, C., Guo, W., Song, Y., Du, J. The genetic type of the oil shale at the northern foot of Bogda Mountain, Xinjiang and prediction for favorable areas. *Journal of Jilin University: Earth Science Edition*, 2006, **36**(6), 950–953 (in Chinese with English abstract).
  10. Bai, Y. Prospects for development of oil shale deposits in southeastern margin of Junggar Basin. *Xinjiang Petroleum Geology*, 2008, **29**(4), 462–465 (in Chinese with English abstract).
  11. Li, J., Dong, D., Chen, G. Prospects and strategic position of shale gas resources in China. *Natural Gas Industry*, 2009, **29**(5), 11–16 (in Chinese with English abstract).
  12. Li, J., Tao, S., Liu, X. Element geochemical characteristics and implications on sedimentary environments of southern Bogda Mountain oil shale. *Clean Coal Technology*, 2012(1), 102–112 (in Chinese with English abstract).
  13. Peng, X., Wang, L., Jiang, L. Analysis of sedimentary environment of the Permian Lucaogou Formation in southeastern margin of the Junggar Basin. *Journal of Xinjiang University: Natural Science Edition*, 2011, **28**(4), 395–400 (in Chinese with English abstract).
  14. Carroll, A. R. Upper Permian lacustrine organic facies evolution, Southern Junggar Basin, NW China. *Org. Geochem.*, 1998, **28**(11), 649–667.
  15. Song, C. *Sedimentary System and Sedimentary Features of Central Junggar Basin*. Geological Publishing House, Beijing, 2006 (in Chinese with English abstract).
  16. Carroll, A. R., Graham, S. A., Smith, M. E. Walled sedimentary basins of China. *Basin Res.*, 2010, **22**(1), 17–32.
  17. XBGMR. *Geological Map* (scale 1:200000), Urumqi sheet (k-45-4), 1965.
  18. Choulet, F., Chen, Y., Wang, B., Faure, M., Cluzel, D., Charvet, J., Lin, W., Xu, B. Late Paleozoic paleogeographic reconstruction of Western Central Asia based upon paleomagnetic data and its geodynamic implications. *J. Asian Earth Sci.*, 2011, **42**(5), 867–884.
  19. Wu, Q. Structural evolution and prospects of Junggar basin. *Xinjiang Geology*, 1986, **4**(3), 1–19 (in Chinese with English abstract).
  20. Wartes, M. A., Carrol, A. R., Greene, T. J. Permian sedimentary record of the Turpan-Hami basin and adjacent regions, northwest China: Constraints on postamalgamation tectonic evolution. *Geol. Soc. Am. Bull.*, 2002, **114**(2), 131–152.
  21. Yang, X., He, D., Wang, Q., Tang, Y. Tectonostratigraphic evolution of the Carboniferous arc-related basin in the East Junggar Basin, northwest China: Insights into its link with the subduction process. *Gondwana Res.*, 2012, **22**(3–4), 1030–1046.
  22. Fang, S., Jia, C., Guo, Z., Song, Y., Xu, H., Liu, L. New view on the Permian evolution of the Junggar Basin and its implications for tectonic evolution. *Earth Science Frontiers*, 2006, **13**(3), 108–121 (in Chinese with English abstract).

23. Tang, W., Zhang, Z., Li, J., Li, K., Chen, Y., Guo, Z. Late Paleozoic to Jurassic tectonic evolution of the Bogda area (northwest China): Evidence from detrital zircon U–Pb geochronology. *Tectonophysics*, 2014, **626**, 144–156.
24. Zhao, B. Nature of basement of Junggar Basin. *Xinjiang Petroleum Geology*, 1992, **13**(2), 95–99 (in Chinese with English abstract).
25. Sun, Z., Shen, J. Bogda nappe structure and its relations to hydrocarbon in Xinjiang. *Petroleum Geology & Experiment*, 2014, **36**(4), 429–434 (in Chinese with English abstract).
26. Tribouvillard, N., Algeo, T. J., Lyons, T., Riboulleau, A. Trace metals as palaeoredox and paleoproductivity proxies: an update. *Chem. Geol.*, 2006, **232**(1–2), 12–32.
27. Alkhafaji, M. W., Aljubouri, Z. A., Aldobouni, I. A. Depositional environment of the Lower Silurian Akkas hot shales in the Western Desert of Iraq: Results from an organic geochemical study. *Mar. Petrol. Geol.*, 2015, **64**, 294–303.
28. Liu, X., Wang, N. *Fish Fossil of Late Permian in Junggar Basin*. Science Press, Beijing, 1978, 1–18 (in Chinese).
29. Di, G. *Petroleum Geology of China*. Volume 15. Hydrocarbon generation area in Xinjiang. Petroleum Industry Press, Beijing, 1993, 65 (in Chinese).
30. Liu, S. Middle Permian conchostracans in Xinjiang. *Acta Palaeontologica Sinica*, 2000, **40**(1), 61–66 (in Chinese with English abstract).
31. Jiao, Y., Wu, L., He, M., Maison, R., Wang, M., Xu, Z. Occurrence, thermal evolution and primary migration processes derived from studies of organic matter in the Lucaogou source rock at the southern margin of the Junggar Basin, NW China. *Sci. China Ser. D-Earth Sci.*, 2007, **50**(Supplement 2), 114–123.
32. Mukhopadhyay, P. K., Wade, J. A., Kruger, M. A. Organic facies and maturation of Jurassic/Cretaceous rocks, and possible oil-source rock correlation based on pyrolysis of asphaltenes, Scotian Basin, Canada. *Org. Geochem.*, 1995, **22**(1), 85–104.
33. Espitalié, J., Madec, M., Tissot, B., Mennig, J., Leplat, P. Source rock characterization method for petroleum exploration. In: *Proceedings of the 9th Offshore Technology Conference*, May 2–5, Houston, Texas, 1977, 439–444.
34. Langford, F. F., Blanc-Valleron, M.-M. Interpreting Rock-Eval pyrolysis data using graphs of pyrolyzable hydrocarbons vs. total organic carbon. *AAPG Bull.*, 1990, **74**(6), 799–804.
35. Dembicki, H. Three common source rock evaluation errors made by geologists during prospect or play appraisals. *AAPG Bull.*, 2009, **93**(3), 341–356.
36. He, D., Chen, X., Zhang, Y., Kuang, J., Shi, X., Zhang, L. Enrichment characteristics of oil and gas in Junggar Basin. *Acta Petrolei Sinica*, 2004, **25**(3), 1–10 (in Chinese with English abstract).
37. Hou, D., Feng, Z. *Petroleum Geochemistry*. China University of Geoscience Press, Wuhan, 2011, 178–243 (in Chinese).
38. Gelpi, E., Schneider, H., Mann, J., Oró, J. Hydrocarbons of geochemical significance in microscopic algae. *Phytochemistry*, 1970, **9**(3), 603–612.
39. Wang, Y., Fang, X., Zhang, T., Li, Y., Wu, Y., He, D., Wang, Y. Predominance of even carbon-numbered *n*-alkanes from lacustrine sediments in Linxia Basin, NE Tibetan Plateau: Implications for climate change. *Appl. Geochem.*, 2010, **25**(10), 1478–1486.
40. Moldowan, J. M., Seifert, W. K., Gallegos, E. J. Relationship between petroleum composition and depositional environment of petroleum source rock. *AAPG Bull.*, 1985, **69**(8), 1255–1268.

41. Ficken, K. J., Li, B., Swain, D. L., Eglinton, G. An *n*-alkane proxy for the sedimentary input of submerged/floating freshwater aquatic macrophytes. *Org. Geochem.*, 2000, **31**(7–8), 745–749.
42. Sachsenhofer, R. F., Bechtel, A., Kuffner, T., Rainer, T., Gratzner, R., Sauer, R., Sperl, H. Depositional environment and source potential of Jurassic coal-bearing sediments (Gresten Formation, Hoflein gas/condensate field, Austria). *Petrol. Geosci.*, 2006, **12**(2), 99–114.
43. Riboulleau, A., Schnyder, J., Riquier, L., Lefebvre, V., Baudin, F., Deconinck, J.-F. Environmental change during the Early Cretaceous in the Purbeck-type Durlston Bay section (Dorset, Southern England): A biomarker approach. *Org. Geochem.*, 2007, **38**(11), 1804–1823.
44. Xie, S., Yao, T., Kang, S., Duan, K., Xu, B., Thompson, L. G. Climatic and environmental implications from organic matter in Dasuopu glacier in Xixiawangma in Qinghai-Tibetan Plateau. *Sci. China Ser. D-Earth Sci.* 1999, **42**(4), 383–391.
45. Xie, S., Evershed, R. P. Peat molecular fossils recording paleoclimatic change and organism replacement. *Chin. Sci. Bull.*, 2001, **46**(20), 1749–1752.
46. Xie, S., Yi, Y., Liu, Y., Gu, Y., Ma, Z., Lin, W., Wang, X., Liu, G., Liang, B., Zhu, Z. The Pleistocene vermicular red earth in South China signaling the global climatic change: The molecular fossil record. *Sci. China Ser. D-Earth Sci.* 2003, **46**(11), 1113–1120.
47. Wang, Z., Liu, Z., Yi, Y., Xie, S. Features of lipids and their implications in modern soils from various climate vegetation zones. *Acta Pedologica Sinica*, 2003, **40**(6), 967–970 (in Chinese with English abstract).
48. Shanmugam, G. Significance of coniferous rain forests and related organic matter in generating commercial quantities of oil, Gippsland Basin, Australia. *AAPG Bull.*, 1985, **69**(8), 1241–1254.
49. Peters, K. E., Walters, C. C., Moldowan, J. M. *The Biomarker Guide*. Volume 2. Biomarkers and Isotopes in Petroleum Exploration and Earth History. Cambridge University Press, Cambridge, 2005, 483–625.
50. Ten Haven, H. L., Rohmer, M., Rullkötter, J., Bissert, P. Tetrahymanol, the most likely precursor of gammacerane, occurs ubiquitously in marine sediments. *Geochim. Cosmochim. Ac.*, 1989, **53**(11), 3073–3079.
51. Connan, J. Molecular geochemistry in oil exploration. In: *Applied Petroleum Geochemistry* (Bordenave, M. L., ed.), Editions Technip, Paris, 1993, 175–204.
52. Sinninghe Damsté, J. S., Kenig, F., Koopmans, M. P., Köster, J., Schouten, S., Hayes, J. M., De Leeuw, J. W. Evidence for gammacerane as an indicator of water column stratification. *Geochim. Cosmochim. Ac.*, 1995, **59**(9), 1895–1900.
53. Seifert, W. K., Moldowan, J. M., Jones, R. W. Application of biological marker chemistry to petroleum exploration. In: *Proceedings of the Tenth World Petroleum Congress*, 9–14 September 1979, Bucharest, Romania. World Petroleum Congress, 1980, SP8.
54. Mackenzie, A. S., Beaumont, C., McKenzie, D. P. Estimation of the kinetics of geochemical reactions with geophysical models of sedimentary basins and applications. *Org. Geochem.*, 1984, **6**, 875–884.
55. Seifert, W. K., Moldowan, J. M., Smith, G. W., Whitehead, E. W. First proof of structure of a C<sub>28</sub>-pentacyclic triterpane in petroleum. *Nature*, 1978, **271**(5644), 436–437.

56. Kong, Q., Zhou, H., Li, T., Chen, W. The discussion of biomarker index. *Journal of Daqing Petroleum Institute*, 1987, 3, 9–15 (in Chinese with English abstract).
57. Huang, W., Meinschein, W. G. Sterols as ecological indicators. *Geochim. Cosmochim. Ac.*, 1979, **43**(5), 739–745.
58. Volkman, J. K. A review of sterol markers for marine and terrigenous organic matter. *Org. Geochem.*, 1986, **9**(2), 83–99.
59. Fowler, M. G., Douglas, A. G. Saturated hydrocarbon biomarkers in oils of Late Precambrian age from Eastern Siberia. *Org. Geochem.*, 1987, **11**(3), 201–213.
60. Seifert, W. K., Moldowan, J. M. Use of biological markers in petroleum exploration. In: *Methods in Geochemistry and Geophysics*, Vol. 24 (Johns, R. B., ed.). Elsevier, Amsterdam, 1986, 261–290.
61. Cardoso, J. N., Chicarelli, M. I. The organic geochemistry of the Paraiba Valley and Maraú oil-shales. In: *Advances in Organic Geochemistry* (Bjoroy, M. et al., eds.), 1981. Wiley & Sons, 1983, 828–833.
62. Albaigés, J., Algaba, J., Grimalt, J. Extractable and bound neutral lipids in some lacustrine sediments. *Org. Geochem.*, 1984, **6**, 223–236.
63. Rieley, G., Collier, R. J., Jones, D. M., Eglinton, G., Eakin, P. A., Fallick, A. E. Sources of sedimentary lipids deduced from stable carbon-isotope analyses of individual compounds. *Nature*, 1991, **352**(6334), 425–427.
64. Ying, G., Fan, P. Origin of aldehydes in sediments of Qinghai Lake. *Sci. China, Ser. B*, 1993, **36**(4), 507–512 (in Chinese).
65. Xu, S. *Organic Chemistry*. Higher Education Press, Beijing, 1982, 293–307 (in Chinese).
66. Tuo, J., Zhang, M., Wang, X. The content and significance of fatty acid methyl esters in Dongsheng sedimentary uranium ore deposits, Ordos basin, China. *Acta Sedimentologica Sinica*, 2006, **24**(3), 432–439 (in Chinese with English abstract).
67. Kolattukudy, P. E. Biopolyester membranes of plants: cutin and suberin. *Science*, 1980, **208**(4447), 990–1000.
68. McMurry, J., Simanek, E. *Fundamentals of Organic Chemistry*. 6th edition. Cengage Learning, 2006, 246–292.
69. Deines, P. The isotopic composition of reduced organic carbon. In: *Handbook of Environmental Isotope Geochemistry* (Fritz, P., Fontes, J. C., eds.). Vol. 1. The Terrestrial Environment. Elsevier, Amsterdam, 1980, 329–406.
70. O’Leary, M. H. Carbon isotopes in photosynthesis. *Bioscience*, 1988, **38**(5), 328–336.
71. Farquhar, G. D., Ehleringer, J. R., Hubick, K. T. Carbon isotope discrimination and photosynthesis. *Annu. Rev. Plant Physiol. Plant Mol. Biol.*, 1989, **40**, 503–537.
72. Liu, W., Li, X., An, Z., Xu, L., Zhang, Q. Total organic carbon isotopes: A novel proxy of lake level from Lake Qinghai in the Qinghai-Tibet Plateau, China. *Chem. Geol.*, 2013, **347**, 153–160.
73. Duan, Y., Ma, L. Several problems concerned with stable carbon isotopic geochemistry of biomarker compounds. *Advances in Earth Science*, 1996, **11**(4), 356–361 (in Chinese with English abstract).
74. Zhang, X. Regional stratigraphic chart of northwestern China, branch of Xinjiang Uygur Autonomous Region. Geological Publishing House, Beijing, 1981 (in Chinese).

75. Hu, Y. Characteristics of the Permian floras in the western part of China. *Regional Geology of China*, 1985, **12**(2), 99–108 (in Chinese with English abstract).
76. Liao, Z., Lu, L., Jiang, N., Xia, F., Sun, F., Zhou, Y., Li, S., Zhang, Z. Carboniferous and Permian in the western part of eastern Tianshan Mountains: In: *Eleventh International Congress of Carboniferous Stratigraphy and Geology*, August 31–September 4, 1987, Beijing, (Liao, Z., ed.), 1987, **4**, 50.
77. Ziegler, A. M., Phytogeographic patterns and continental configurations during the Permian Period. In: *Palaeozoic Palaeogeography and Biogeography* (McKerrow, W. S., Scotese, C. R., eds.). Geological Society Memoir, 1990, **12**(1), 363–379.

*Presented by J. Qian and A. Soesoo*

Received June 15, 2015